V.I. SOROKA,[1] S.O. LEBED,[2,3] M.G. TOLMACHOV,[2] O.G. KUKHARENKO,[2,3] O.O. VESELOV[2]

[1] Institute for Nuclear Research, Nat. Acad. of Sci. of Ukraine
(47, Nauky Ave., Kyiv 03680, Ukraine; e-mail: soroka@kinr.kiev.ua)
[2] Laboratory "Spectrum", TMM Ltd
(50a, Mashynobudivna Str., Kyiv 03148, Ukraine)
[3] Laboratory "TIMS", Institute of High Technologies,
Taras Shevchenko National University of Kyiv
(50a, Mashynobudivna Str., Kyiv 03148, Ukraine)

PACS 34.50.Dy, 79.20.Rf, 85.35.-p, 82.80.Yc

NUCLEAR MICROANALYSIS STUDY OF SURFACE NANOLAYERS IN GOLD–SILICON STRUCTURES

The Rutherford backscattering and particle-induced X-ray emission methods are used to study the surface layers in gold–silicon structures, the parameters of which govern the operational characteristics of electron devices constructed on their basis. The measurements are performed on a high-precision micro-analytical unit "Nuclear scanning probe" recently put into operation at the "Spectrum" laboratory. The thicknesses of a gold layer sputtered onto the specimen surface were about 17 and 20 nm for two different specimens. The layer non-uniformity was less than 1.6 nm and did not exceed the experimental error. A substantial amount of the fluorine impurity was revealed under the gold layer in the gold–silicon interface layer. Probably, it may be remnants of fluorine remaining after the etching of the silicon surface in a mixture of acids that included the hydrofluoric one (HF). The amount of fluorine detected in a series of measurements was found to strongly correlate with the current of alpha-particles at the target surface during the spectrum measurement. Since the local heating of the target depends on the current, it is evident that the local diffusion rate of fluorine atoms varied over the target surface.

Keywords: nuclear microanalysis, Rutherford backscattering, particle induced X-ray emission, alpha particles, "Nuclear scanning probe", surface layers, interface layer.

1. Introduction

A considerable number of works are devoted to the study of barrier structures owing to their wide application in micro- and nanoelectronic devices. Special attention is focused on the researches of metal–semiconductor interface layers, which substantially govern the electrophysical properties of those devices. The interface between contacting materials depends on the way of its formation. The fabrication technologies for various types of heterosystems include many routine operations. However, for the process of barrier structure formation, two stages are crucial. These are the stage of semiconductor surface preparation (especially, its final phases–etching, washing, and drying) and the stage of surface metallization (especially, the phases of metal deposition onto the surface and the thermal treatment).

The purpose of this research consisted in checking some results obtained at two indicated stages of the Au/Si structure fabrication after certain modifications of the corresponding technology had been introduced. At the same time, the work aimed at testing the functionalities of a high-precision microanalyti-

© V.I. SOROKA, S.O. LEBED, M.G. TOLMACHOV, O.G. KUKHARENKO, O.O. VESELOV, 2013

Table 1. **Analytical capabilities of nuclear physical techniques implemented on a scanning nuclear microprobe in Kyiv**

Method	Measured signal	Spatial resolution, μm	Depth resolution, μm	Detected elements (atomic number, Z)	Threshold sensitivity, mg/kg	Error of quantitative analysis, %
PIXE	X-rays	$\geq$2.0	0.5–15	>11	~1	5–10
RBS	Backscattered ions	$\geq$2.0	0.01–15	>2	~1	3–5

cal unit "Scanning nuclear probe" that had been recently put into operation [1, 2]. In our researches, we used analytical methods of nuclear physics, namely, the methods of nuclear microanalysis. More specifically, these are the Rutherford backscattering (RBS) method [3] and the method of characteristic x-ray emission induced by accelerated particles (particle-induced x-ray emission, PIXE) [4].

2. Experimental Part

Measurements were carried out on an original installation "Scanning nuclear microprobe" based on a modernized single-ended electrostatic ion accelerator KN-3000 of the Van de Graaff type [1, 2]. The major electrotechnical parameters of this installation are as follows:

– accelerated particles are protons and alpha-particles (ions of hydrogen and helium atoms);

– ion beam energy is 1 to 2.2 MeV;

– current of the working ion microbeam at a studied specimen is 1 pA to 15 nA (for the average diameter of a beam spot on the specimen from 2 to 50 μm, respectively);

– maximum area of microbeam scanning is 400×400 μm^2;

– residual gas pressure in the vacuum chamber of targets is 10^{-7} to 10^{-6} Torr.

For today, two experimental techniques for the accelerator have been elaborated and testified. These are the PIXE and RBS methods (see Table 1). Together, they allow both the qualitative and quantitative (including two-dimensional) microanalyses of dominant, impurity, and trace chemical elements in specimens to be executed. If necessary, those techniques can be applied simultaneously. Some advantages of micro-RBS and micro-PIXE techniques over alternative microanalytical methods should also be emphasized:

– a high threshold sensitivity (down to 1 mg/kg) for the majority of chemical elements;

– applicability to the analysis of almost all elements;

– express analysis (from 5 to 100 min);

– a high resolution both over the surface and into the depth of a specimen (see Table 1);

– non-destructive analysis.

Table 1 demonstrates that both methods complement well each other. Having approximately the same sensitivity, the former is almost absolutely selective with respect to chemical elements, whereas the latter has a better resolution in depth and is capable of analyzing the light elements (with $Z > 2$) in the specimen as well.

From a batch of specimens, two were selected for the research. At the initial stage of the experiment, only one task was formulated, namely, to measure the thickness of a gold layer sputtered onto the silicon surface. In addition, it was necessary to determine the thickness at several points in order to estimate the non-uniformity of the profile of this layer over the surface. The line of points, in vicinities of which the measurements were carried out, passed through the target center. The RBS experiment was carried out on the standard setup, when the direction of the beam from the accelerator, after passing a 90° analyzing magnet, coincided with the normal to the target surface. The scattering angle θ was 157°. Some measurements were carried out in a geometry with inclination, when the angle θ_1 between the beam direction and the normal to the target was equal to 60° provided the same scattering angle.

In this experiment, the RBS spectra were obtained with the help of a silicon surface-barrier detector and with the use of alpha-particles with an energy of 1.85 MeV. To calibrate the energy scale of an analyzer and some other testings, the energy was reduced to 1.5 MeV. The energy scale of the analyzer chan-

nel was set at a level of 4.34 keV/channel. Spectra for separate points were accumulated at various values of alpha-particle current at the target. The current was varied approximately from 2.5 nA to 12.0 nA.

X-ray radiation was registered using an energy-dispersive Si(Li) detector with an energy resolution of 165 eV at a radiation energy of 6 keV. The PIXE detector was arranged at an angle of about 60° with respect to the direction of the ionic beam from the accelerator.

The spectra in Fig. 1 partially illustrate the capabilities of the methods under consideration concerning the identification of chemical elements in the near-surface layers of the target. The both spectra were obtained under identical conditions: the energy of α-particles, E_0, was 1.50 MeV, and the scattering angle was 157°. The lower spectrum corresponds to the scattering at a surface of silicon specimens covered with a gold layer. The upper spectrum was registered at the scattering from the rear side of the same silicon specimen, but covered with a germanium layer.

The kinematic factor (the right ordinate axis) for the given experimental conditions can be calculated by the known formula or by using the interpolated tabular data [3]. For elements Au and Si, which are unquestionably present in the target, this factor equals 0.9252 and 0.5805, respectively. The coordinates of the cross marked as Au correspond to the kinematic factor and the number of an analyzer channel for the weight center of the gold peak. The coordinates of the cross marked as Si correspond to the kinematic factor and the half-height of the front edge of the spectrum registered from silicon. The linear dependence of the energy of scattered particles (the analyzer channel number) on the kinematic factor allows a straight line Au–Si to be drawn and extrapolated. The line slope is set by the energy scale of an analyzer channel. Now, it becomes clear that the intersection between the coordinate line of the peak weight center registered in approximately the 135-th channel and the drawn line enables the kinematic factor of unknown element to be determined. Its value, $K = 0.445$, corresponds to the chemical element fluorine, F^{19}. Using the same technique, we registered–approximately in the 105-th channel–the scattering at the surface layer of oxygen (O^{16}, $K = 0.381$). One more cross in the plotted line marks the position of germanium. However, the decoding of PIXE spectra in this case unambiguously testifies to the presence,

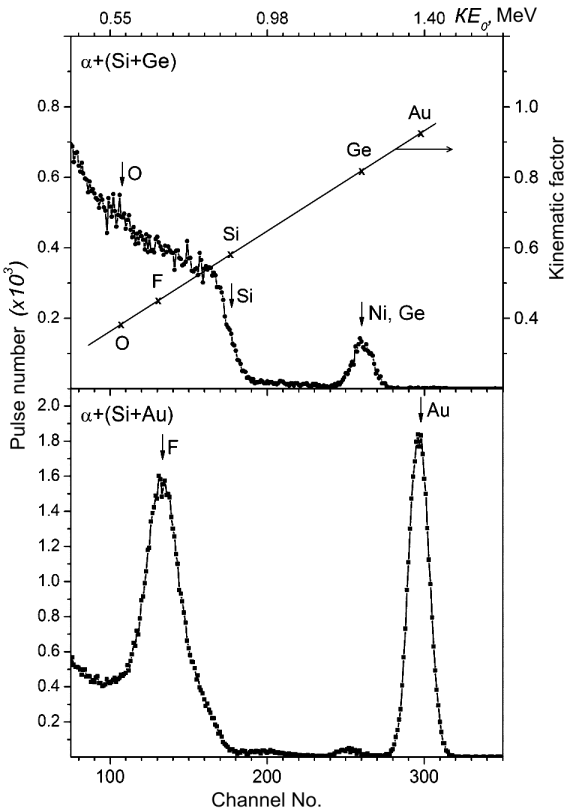

Fig. 1. Backscattering spectra of 1.50-MeV α-particles at an angle of 157°. Crosses denote the peak positions of chemical elements and the position of the high-energy edge of the silicon spectrum in accordance with their kinematic factor

besides germanium atoms, of nickel atoms as well. Since germanium and nickel are approximately in the middle of the periodic system of elements and close to each other, their signals in the RBS spectrum are practically unresolved under the given experimental conditions.

3. Results

Figure 2 illustrates some backscattering spectra obtained for α-particles with an energy of 1.85 MeV under different experimental conditions. One can see that, in addition to the well-pronounced peak formed by α-particles scattered at a thin gold layer, the spectra reveal another peak. It is superimposed on the high-energy part of the scattering spectrum registered from the thick silicon matrix. When the energy of α-particles was varied, both the peak shape and its relative position remained the same (Figs. 1 and 2).

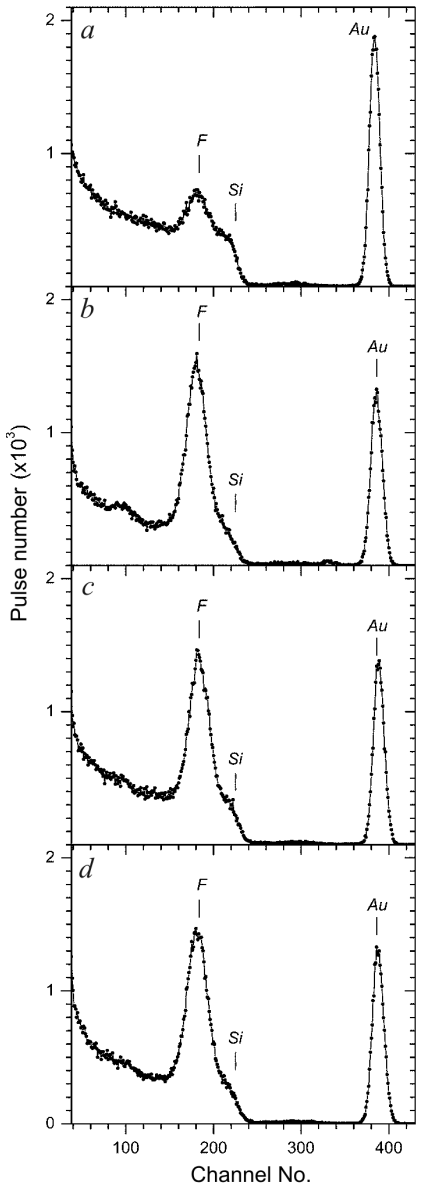

Fig. 2. RBS spectra from the fragments of the working specimen surface under various experimental conditions: (*a*) specimen 1, $\theta = 157°$, $\theta_1 = 0°$, $I = 12$ nA; (*b*) specimen 2, $\theta = 157°$, $\theta_1 = 0°$, $I = 2.5$ nA; (*c*) specimen 1, $\theta = 157°$, $\theta_1 = 0°$, $I = 2.5$ nA; (*d*) specimen 1, $\theta = 0°$, $\theta_1 = 60°$, $I = 2.5$ nA

Hence, the peak was not induced by the resonant nuclear interaction, but was a result of the Rutherford scattering by an element lighter than silicon. Additional measurements (provided the standard geometry and the geometry with inclination at the same point on the target surface) showed that the unknown element is located in the near-surface region of silicon. The corresponding calculations allowed this chemical element to be identified as fluorine, F^{19}. (Here, it is worth noting that an analogous experiment revealed no traces – at all! – of fluorine atoms in a gold–silicon specimen fabricated earlier using a somewhat different technology.) Small spectral peaks observed in the interval near the 100-th channel correspond to the kinematics of α-particle scattering by the carbon surface layer. A carbon deposit accumulated on the target surface during its irradiation with α-particles is connected with the presence of remnants of oil vapor from the molecular pump inserted while evacuating the reaction chamber.

For a reliable identification of fluorine atoms, it was necessary firstly to determine the thickness of the gold surface layer, in order to make allowance for the energy losses of α-particles at their passage through gold in both the forward (particles from the accelerator) and backward (scattered particles) directions. Omitting the detailed calculations of the RBS theory [3], let us write down the final formula for the thickness of a heavy-element layer on the surface of a light-element matrix,

$$(Nt)_i = \frac{A_i}{H_M}\frac{\sigma_M}{\sigma_i}\frac{\delta E}{\left[\varepsilon_M^M\right]}, \qquad (1)$$

where $(Nt)_i$ is the number of heavy element atoms per 1 cm^2 (the layer thickness is expressed in terms of the number of atoms per unit area); N is the atomic concentration of the chemical element; t the layer thickness expressed in terms of length units; A_i the spectral area (in counts) of the signal under the peak of the examined element (Fig. 1); H_M the spectrum height equal to the number of counts in the analyzer channel for the scattering from the matrix surface; σ_M the cross-section of Rutherford scattering at matrix nuclei; σ_i the cross-section of Rutherford scattering at nuclei of the studied element; δE the analyzer channel width; and $\left[\varepsilon_M^M\right]$ the backscattering factor corresponding to the scattering atom and the substance, in which α-particles are slowed down (to simplify the calculations, it is possible to use the corresponding factor values from the available tables [3]). Note that formula (1) was derived for a small thickness of the surface layer (or a small number of atoms in the near-surface layer of the matrix). However, the criterion of "smallness" was not specified.

The differential cross-sections for the elastic scattering of charged particles with charge Z_1 by the Coulomb field of a nucleus with charge Z_2 are given by the Rutherford formula. For small ratios m/M, where m is the mass of an incident particle, and M is the mass of a scattering atom, this formula has a convenient approximation,

$$\frac{d\sigma}{d\Omega} \cong 1.295 \left(\frac{Z_1 Z_2}{E_0}\right)^2 \times$$
$$\times \left[\mathrm{cosec}^4 \frac{\theta}{2} - 2\left(\frac{m}{M}\right)^2 + ...\right], \text{ mbarn/sr}, \qquad (2)$$

where the energy is expressed in the MeV units.

Figure 3 illustrates the dependence of the thickness of the gold layer on the specimen surface on the place of its measurement. We may assert that, for the average thickness of about 17 nm for specimen 1 and about 20 nm for specimen 2, the thickness nonuniformity does not exceed the experimental error. The average statistical error for the layer thickness (the total width at the half-height of the distribution) amounted to about 1.6 nm. While changing from measuring the gold layer thickness in the atom/cm^2 units to linear ones (nm), we supposed that the atomic concentration in the near-surface layer was equal to that in the substance bulk. It is worth noting that this result agrees with estimations concerning the measurements of the gold layer thickness uniformity by the spectrophotometric technique at the stage of specimen fabrication.

To calculate the number of fluorine atoms, we also used formula (1). The fluorine peak can be pronouncedly distinguished against the scattering background from silicon. The total number of counts under the fluorine peak, A_i, was determined by subtracting the counts of scattering by silicon in the corresponding analyzer channels. Of course, using this way of calculation, some systematic error was inserted. For the backscattering factor $[\varepsilon]$ to be determined more exactly, one should take into account that we study a layer composed of two elements, silicon and fluorine, in a certain ratio. However, in the discussed experiment, we were interested, first of all, in the very fact of the presence of fluorine and in its relative concentration on the surface.

The results of measurements of the fluorine amount $(Nt)_\mathrm{F}$ at the same places of the specimen surface, where we studied the gold layer, are shown in Fig. 4.

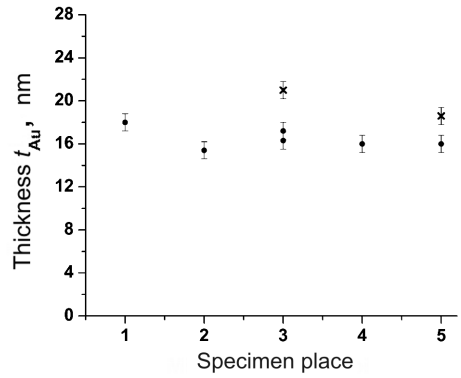

Fig. 3. Thicknesses of the gold surface layer at some points on the working specimen surface for specimen 1 (circles) and 2 (crosses). The measurements were carried out along a line passed through the specimen center (place 3). Places 1 and 5 were taken at the specimen edges

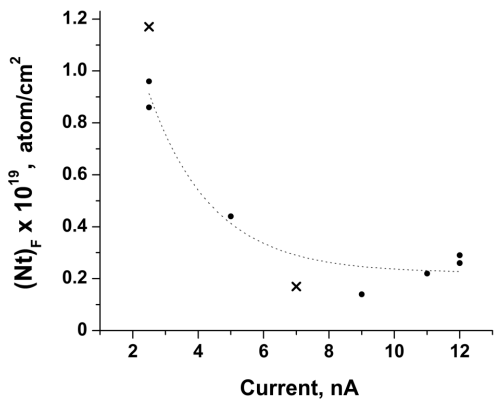

Fig. 4. The dependences of the surface concentration of fluorine atoms in the near-surface layer of silicon on the α-particle current for specimen 1 (circles) and 2 (crosses)

We focus attention on the interesting fact that the determined number of fluorine atoms correlates very strongly with the magnitude of α-particle current used at the measurements of their scattering at the selected places on the specimen surface. So, the questions arise: Which is the origin of fluorine available in such an amount? and Why does it behave itsef so? One of the operations applied at the stage of specimen preparation was, after grinding a silicon workpiece, its etching in a mixture of acids. The mixture included, in particular, the concentrated fluoric (hydrofluoric) acid. Hydrogen fluoride and hydrofluoric acid interact with silicon dioxide SiO_2 [5],

$$SiO_2 + 4HF = SiF_4 + 2H_2O. \qquad (3)$$

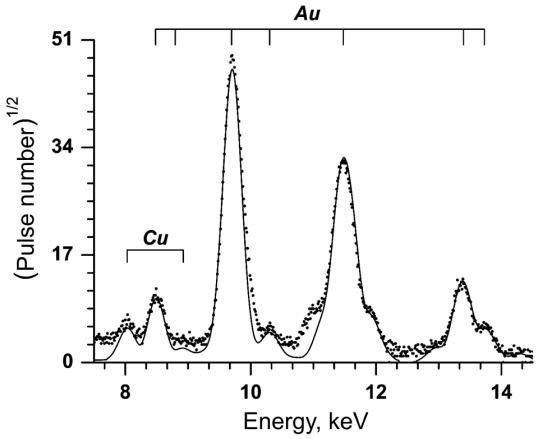

Fig. 5. PIXE spectrum for a fragment of the working surface of specimen 2

As a result, gaseous silicon fluoride, SiF_4, is formed. Silicon fluoride is not released in the fluoric acid solution, because it interacts with HF molecules,

$$SiF_4 + 2HF = H_2[SiF_6], \quad (4)$$

to form the well soluble fluosilicic acid, and the silicon atom in every molecule of this acid is strongly bound with six fluorine atoms. Therefore, if the etching operation was not properly followed by the washing and drying procedures, the acid remnants might remain substantial.

The near-surface layers of researched specimens may also contain a small amount of oxygen, which is usually washed out by the fluoric acid. However, its signal falls in the low-energy region of a large fluorine peak and is practically indistinguishable in the spectra (Fig. 1). As to hydrogen, the scattering of α-particles by hydrogen atoms at backward angles is impossible kinematically.

Now, let us analyze the dependence of the revealed quantity of fluorine on the α-particle current applied at the specimen study. The calculations show that, at a current of 10 nA, a power of 1.85×10^{-2} W was released in the course of 1.85-MeV particle deceleration. Note that the area of irradiated section on the target surface was equal to 2×10^{-5} cm^2 (the diameter of the beam on the target surface was approximately 50 μm). Being recalculated to an area of 1 cm^2, the released power is equivalent to about 1 kW. Hence, the local heating of the target was considerable. Probably, it may be enough for the fluorine atoms to intensively diffuse from the specimen surface. It is of interest that, when the α-particle current was diminished by approximately a factor of 5, the diffusion intensity appreciably fell down. It is expedient to analyze this phenomenon from various aspects.

It is known [6] that the cross-sections of PIXE reactions at protons are much larger than those at α-particles for the majority of chemical elements. Therefore, for the PIXE analysis of specimens, we used a microbeam of protons. In Fig. 5, the experimental and calculated PIXE spectra (the lines of K and L series for Cu and Au, respectively) are shown for the fragment of the working surface in the central part of specimen 2.

The experimental spectrum was measured in the regime, when a microbeam of 1.85-MeV protons was used in a programmed uniform scanning of the specimen surface 300×300 μm^2 in area in a previously selected region (where the RBS spectrum depicted in Fig. 2, *b* was measured). The microbeam positioning was executed with the help of a mechanic 3D (in the coordinate space) micromanipulator and an optical 500X microscope [1, 2]. The size of a proton beam spot on the specimen surface did not exceed 15 μm, and the current strength was 300 pA. To filter off the intensive low-energy X-rays emitted by the silicon substrate of the specimen, a standard filter – a 40-μm aluminum film – was arranged before the PIXE detector. This way allowed us to avoid the overload of Si(Li) detector and provide a high sensitivity of the technique with respect to heavier chemical elements. The applied means favored the detection of regularly distributed copper remnants in a number of examined zones on the surface of specimen 2 (see Fig. 5). The simulated PIXE spectrum exhibited in this figure was calculated with the help of the world-known software program GupixWin [7]. The program code was used for the subsequent quantitative analysis of spectra. It was found that the concentration of gold in the scanning interval equaled 38.4 μg/cm^2, which is equivalent to a gold film about 20 nm in thickness and agrees well with the results of previous RBS analysis of the specimen. We also calculated the relative, with respect to gold, concentration of copper remnants and obtained a value of 0.21%.

4. Conclusions

Our researches confirmed that nuclear methods of nondestructive analysis can successfully be used not only to study materials, but also products from them.

The monitoring within those methods can provide valuable information at the stage of device manufacture and, occasionally, at the stage of device exploitation. In such a manner, the origin of the degradation of functional characteristics can urgently be revealed.

An electrostatic accelerator, which has recently been put in operation in Kyiv, is equipped with a microprobe and allows two experimental techniques to be applied. It is quite suitable for the fulfillment of a wide class of works dealing with the nuclear microanalysis. Moreover, the first experiments showed ways for the improvement of the accelerated particle beam parameters and the operational characteristics of applied techniques. In combination, the methods allow experiments with a higher precision to be carried out and more exact data to be obtained.

The discovery of a significant amount of fluorine in the interface layer gold–silicon, as well as the fact of a considerable variation of its relative concentration as a function of α-particle current at the stage of spectrum accumulation, needs additional experimental researches. It is also expedient to repeat the quantitative analysis of the calculation results for fluorine in the framework of more correct approximations, because the adopted criterion of "smallness" can be too rough for the revealed number of fluorine atoms.

The authors express their gratitude to Dr. Ja. Lekki (Institute of Nuclear Physics, Kraków, Poland) for his help in carrying out the quantitative PIXE analysis.

1. S. Lebed, M. Tolmachov, O. Kukharenko, and O. Veselov, Nucl. Instrum. Methods B **267**, 2013 (2009).
2. *Scanning ionic probe from the "Spectrum" laboratory*, http://www.prober.in.
3. W.K. Chu, J.W. Mayer, and M.A. Nicolet, *Backscattering Spectrometry* (Academic Press, New York, 1978).
4. S.A.E. Johanson and T.B. Johanson, Nucl. Instrum. Methods B **137**, 473 (1976).
5. N.L. Glinka, *General Chemistry* (Gordon and Breach, New York, 1965).
6. M.B.H. Breese, D.N. Jamieson, and P.J.C. King, *Materials Analysis Using a Nuclear Microprobe* (Wiley, New York, 1996).
7. J. Maxwell, J. Campbell, and W. Teesdale, Nucl. Instrum. Methods B **43**, 218 (1989).

Received 27.08.12.
Translated from Ukrainian by O.I. Voitenko

В.І. Сорока, С.О. Лебедь, М.Г. Толмачев, О.Г. Кухаренко, О.О. Веселов

ДОСЛІДЖЕННЯ МЕТОДАМИ ЯДЕРНОГО МІКРОАНАЛІЗУ ПОВЕРХНЕВИХ НАНОШАРІВ СТРУКТУРИ ЗОЛОТО–КРЕМНІЙ

Р е з ю м е

Ядерними аналітичними методами резерфордівського зворотного розсіяння та індукованого частинками характеристичного рентгенівського випромінювання досліджено поверхневі наношари структури золото–кремній. Від параметрів цих шарів кардинально залежать електротехнічні властивості побудованих на їх основі електронних приладів. Вимірювання виконано на прецизійній мікроаналітичній установці "Скануючий ядерний зонд" щойно введеній в експлуатацію в лабораторії "Спектр". Експеримент показав, що товщина шару золота, напиленого на поверхню зразків, дорівнює ∼17 нм (для одного зразка) і ∼20 нм (для другого зразка). Неоднорідність товщини цих шарів по поверхні не перевищує 1,6 нм і не виходить за межі похибки експерименту. Під золотом, у проміжному шарі золото–кремній, виявлено значну кількість домішки. Імовірно, що це залишок фтору після технологічної операції травлення поверхні кремнію в суміші кислот, куди входить і плавикова (HF) кислота. Показово, що кількість виявленого фтору для серії вимірів сильно корелює з величиною струму альфа-частинок на мішені під час набору спектра. Очевидно, що локальний нагрів мішені залежить від величини струму. Звідси випливає різна швидкість локальної дифузії атомів фтору з поверхні мішені.